Microporous and Mesoporous Materials 209 (2015) 2-9
doi:10.1016/j.micromeso.2014.10.033

Fast synthesis of micro/mesoporous xerogels: textural and energetic assessment

Elizabeth Isaacs Páez[1,2], Marta Haro[3]*, Emilio J. Juárez-Pérez[3], Rocío J. Carmona[1], José B. Parra[1], Roberto Leyva Ramos[2], Conchi O. Ania[1]*

[1] Instituto Nacional del Carbón, INCAR-CSIC, Apdo. 73, 33080 Oviedo, Spain

[2] Centro de Investigación y Estudios de Postgrado, Facultad de Ciencias Químicas, Universidad Autónoma de San Luis Potosí, México

[3] Photovoltaic and Optoelectronic Devices Group, Dpt. Física, Universitat Jaume I, Castelló, Spain

Abstract

The sol-gel polymerization of resorcinol/formaldehyde mixtures to obtain porous gels is typically a long process performed throughout several days. In this work, we have explored an experimental approach to reduce the time necessary to obtain porous gels based on mild polymerization conditions and direct drying. We have analyzed the effects of the temperature and time of the gelation/aging step on the porosity of the gels, as well as the impact on the overall energetic cost of the process. Data have shown that well-developed micro-mesoporous architectures can be obtained within less than a day. The temperature of the gelation/aging step mainly affects the mesopore network, whereas the microporosity is determined by the composition of the precursor's mixture. The exclusion of the solvent exchange step yields soft mechanically fragile porous gels with structural limitations upon carbonization at high temperature in inert atmosphere, due to the surface tensions applied to the backbone during the evolution of volatiles. The mesopore structure lost during carbonization is not recovered upon activation in CO_2 atmosphere, but it is preserved upon chemical activation in K_2CO_3 and the resulting gel exhibits a bimodal micro-mesoporous distribution. Furthermore, the energy savings of this route are similar to those obtained using microwave-heating in terms of grams of xerogel per kilowatt hour of energy consumed for similar textural properties. The correlation between the energy power consumed and the textural parameters is a useful tool to optimize the synthesis.

*Corresponding author: C.O. Ania, Instituto Nacional del Carbón, INCAR-CSIC, Apdo. 73, 33080 Oviedo, Spain, Tel/Fax: +34 985 118846/ +34 985 297662; M. Haro, Photovoltaic and Optoelectronic Devices Group, Dept. Física, Universitat Jaume I, Castelló, Spain, Tel/Fax: +34 985 118846/ +34 985 297662. E-mail address: conchi.ania@incar.csic.es (C.O. Ania); mharo@uji.es (M. Haro)

1. Introduction

Driven by the need to obtain highly featured materials with controlled properties, the synthesis of micro-mesoporous materials with tailored surface areas and pore volumes, and uniform pore sizes has become a subject of great interest [1]. Among different options, polymeric organic and carbon gels are postulated as interesting materials in many diverse fields due to their relatively low-cost and unique physical, chemical, and electrochemical properties that may be tuned during the synthesis and processing [2-5]. Industrial applications in sectors such as adsorbents for gas separation [6], catalyst supports [7,8], energy storage devices [9-11], capacitive deionization [12-13] and so forth have been largely studied since the first work of Pekala and coworkers [14].

In these two decades numerous articles have appeared in the literature describing various synthesis and processing conditions and their effects on the final structure (morphology, texture, composition) and performance [2-5,15]. To date most of the synthesis are based upon the catalyzed polycondensation of resorcinol (R)-formaldehyde (F) mixtures in water, although some alternative harmless and naturally available precursors have also been described [16,17]. Optimization of this process is crucial to control the characteristics and performance of the gels, as well as the economic balance for its large-scale implementation.

The sol-gel polycondensation of R-F mixtures in the presence of a catalyst is endothermic, and then heating is required to provide the necessary energy for this reaction. The typical temperature for this reaction in aqueous medium is ca. 80 ºC [2], although it may be decreased when longer gelation times [18] or alternative solvents to water are used [19]. According to literature, the mechanism of formation of R-F gels is initiated by addition reactions between the precursors followed by condensation and cluster growth [3-5]. Dynamic viscosity measurements have shown that the initial cluster formation and particle growth takes about one hour [20]; at this stage, the mixture constitutes a colloidal solution of clusters of monomeric particles. This general mechanism depends on the solution pH, the components molar ratios and the temperature, among others [2]. The next stage is the covalent cross-linking of the clusters until they become unstable and undergo spinodal decomposition leading to the solidification of the gel. The gelation may occur by the second day [21], but it is usually performed for about a week at 80 to 90 ºC to assure a complete cross-linking and to prevent swelling during the drying stage. The simplest and less expensive strategy to remove the aqueous solvent is the subcritical drying at ambient pressure that typically renders a lightweight organic polymer called xerogel. Being economically more advantageous, the main drawback of subcritical drying is the structural collapse of the structurally fragile xerogels that usually cannot withstand the surface tensions arisen during drying (although the process depends on the drying rate and thickness of the sample). As a result of all the steps, the sol-gel polymerization of R-F mixtures is typically a long process performed throughout several days.

Knowing this, the objective of this work was to shorten the long time, usually, required for the preparation of porous xerogels with micro-mesoporous structure. The synthesis of xerogels can be achieved in less than 24 hours by combining mild conditions during the sol-gel polymerization reaction and direct drying. We have analyzed the effect of reducing the temperature and time of the gelation/aging stage on the micro/mesoporous architecture of the xerogels, as well as on their structural stability and resiliency towards the surface tensions arisen during the gas evolution upon carbonization at high temperatures. Additionally, we have evaluated and analyzed the energy consumption of the process at such mild conditions. With these data, a balance of energy costs and final micro-mesopore structure of the xerogels can be discussed and compared to other approaches based on non-conventional heating.

2. Experimental

2.1 Materials synthesis

Porous organic and carbon xerogels were synthesized by the conventional sol-gel polymerization of resorcinol (R) and formaldehyde (F) in water (W), using sodium carbonate (C) as catalyst. Details of the synthesis have been reported elsewhere [12]. Briefly, the precursors (molar ratios R/C 200, R/W 0.06 and R/F 0.5) were mixed under magnetic stirring and immediately heated in airtight sealed glass vessels for gelation/aging at different temperatures (ca. 70, 80, 85, 90, 95ºC) and times (ca. 1, 2, 4, 12 h) in a conventional oven. After completion of the gelation/aging step, the wet gels were dried at subcritical conditions at 150 ºC for 12 h without solvent removal. The organic gels are labeled as OGT-t, where *T* is the temperature of the gelation/aging step and *t* the time in hours. A gelation/aging time of 4 hours was used when no other information is given. Additionally, sample OG80 was further activated to develop the porous structure by physical activation using CO_2 (10 mL/min, 800ºC, 10 h) and chemical activation using K_2CO_3 (300 mL/min N_2, 700ºC, 1 h, ratio gel:K_2CO_3 of 1:3). The sample after carbonization at 800ºC is labeled as CG, and those after physically and chemically activated are labeled as CGPA and CGCA, respectively.

2.2 Nanotextural and Chemical Characterization

The nitrogen adsorption–desorption equilibrium isotherms at -196°C were measured in an ASAP 2020 (Micromeritics) volumetric analyzed on samples previously degassed under dynamic vacuum (ca. 10^{-5} Torr) at 120°C for 17 hours. Strict analysis conditions were programmed during the gas adsorption measurements to ensure equilibrium data, thus the average elapsed time for each isotherm was 90-120 h. Each isotherm measurement was performed in duplicate to guarantee the accuracy of the experiments (error was below 0.1%) and to obtain reproducible data. Ultrahigh purity nitrogen (i.e., 99.9992%) was supplied by Air Products. The isotherms were used to calculate the specific surface area using the Brunauer–Emmett–Teller theory, S_{BET}, total pore volume, V_{TOTAL}, and micropore

volumes using the Dubinin-Radushkevich (DR) equation. The PSD analysis in the full micro-mesopore range was performed using the new 2D-NLDFT-HS model assuming surface heterogeneity of pores [22]. The narrow microporosity was further assessed by CO_2 adsorption isotherms at 0ºC. The skeletal density of the synthesized materials was determined by helium picnometry (true density, ρHe) in an Accupyc 1330 apparatus (Micromeritics) thermostatically controlled with an external circulating bath at 35 ºC. Samples were previously outgassed as indicated earlier. Bulk densities, ρ_{bulk}, were estimated as $\rho_{bulk} = 1 / [V_{TOTAL} + 1/\rho He]$ [23]. Elemental analysis was carried out in LECO CHNS-932 and LECO VTF-900 automatic analyzers. The surface chemistry was characterized by the determination of the pH at the point of zero charge (pH_{PZC}) using the mass-titration procedure, according to the experimental procedure described elsewhere [24].

2.3 Energy consumption and cost assessment

The oven was equipped with an electrical power energy meter to measure the cumulative energy consumed during the gelation/aging and drying steps at the different experimental conditions described above. To balance the textural properties of the xerogels (surface area and pore volume) with the energy power consumed per mass of material, we have considered an average yield of 17 grams of dried gel for an initial volume of 50 mL in a typical synthesis.

3. Results and Discussion

3.1 Effect of gelation/aging time and temperature

We have explored an experimental approach to reduce the long time usually needed for the synthesis of porous xerogels based on the sol-gel polymerization of resorcinol/formaldehyde mixtures reported by Pekala and co-workers [14]. Our modification consisted in using mild polymerization conditions (i.e., temperatures between 70-95ºC), reducing the gelation/aging time (we cannot distinguish between both steps) and eliminating the solvent exchange previous to the drying step, to achieve the synthesis in less than 24 hours. The synthesis conditions (reactants molar ratio, solution pH) were selected based on our previous studies to assure the formation of materials with a well developed micro- and mesoporous structure [11,12]. Also, according to literature the development of the mesoporosity in xero- and aerogels is favored when the reactivity of the precursors is lowered by reducing the amount of catalyst [4,5]. As we have maintained a constant R/C molar ratio of 200 for all the samples, the evolution of the porosity will depend on the gelation/aging temperature and time.

Figs. 1 and 2 show the N_2 adsorption isotherms at -196ºC of the gels prepared at different temperatures and times, while the main textural parameters are compiled in Table 1. It should be first mentioned that we have observed a slight shrinkage of the xerogels (between 15-20%) due to direct drying without solvent removal, although no cracks were visible in the monoliths; this is in agreement with

previous works reported for carbon aerogels [25]. Despite of this, the nitrogen isotherms revealed the porous character of all the materials, confirming that the cross-linking reactions leading to the development of the porosity are sufficiently completed at the low temperatures and short gelation/aging times used. Density values measured from helium picnometry are also in agreement with those typically reported for organic xerogels [2,4,5], while apparent densities vary between 0.8-1.2 g/cc for all the samples (Table 1). Furthermore, the xerogels exhibited type IV isotherms regardless the temperature and time of the gelation/aging step. This also corroborates that despite the accelerated synthesis conditions, interconnected polymeric clusters are formed leading to the development of a mesoporous network. However, substantial differences are observed depending on the gelation/aging conditions, putting forward the impact of both parameters on the development of the porosity of the gels.

Table 1. Porosity parameters obtained from the N_2 adsorption isotherms at -196 ºC for the xerogels.

Fig. 1. (A) Nitrogen adsorption/desorption isotherms at -196 ºC for the series of xerogels prepared by gelation/aging at 70 ºC during different times; (B) cumulative and (C) derivative PSD curves calculated using 2D-NLDFT-HS method.

Fig. 2. (A) Nitrogen adsorption/desorption isotherms at -196 ºC for the series of xerogels prepared by gelation/aging at different temperatures for 4 hours; (B) cumulative and (C) derivative PSD curves calculated using 2D-NLDFT-HS method.

Fig. 1 shows the evolution of the N_2 adsorption isotherms of the series of xerogels prepared at 70 ºC and different times. As seen, the development of the porosity is enhanced with time. Even after 1 hour of reaction, an incipient hysteresis loop is observed in the nitrogen adsorption isotherm of sample OG70-1, indicating that the formation of the mesoporous structure has started. Interestingly, the position of the hysteresis loop remained unchanged for all the samples, although it is better defined at longer times, with almost no difference for samples OG70-4 and OG70-12. Longer times also favored the development of the microporosity, although this effect was less pronounced than for the mesopores. This trend was also corroborated by the assessment of the narrow microporosity by means of CO_2 adsorption isotherms shown in Fig. 3; as seen, the micropore volumes are twice larger when the gelation time increased from 1 to 4 hours.

Fig. 3. CO_2 adsorption isotherms at 0 ºC for the series of synthesized xerogels.

The impact of the gelation/aging time on the micro-mesopore structure of the gels is more clearly seen in Fig. 4. The development of the porous network occurs within the first hours of the reaction, with

values of pore volumes reaching a plateau after 4 hours. No further improvement was observed when the synthesis was carried out for 12 hours or several days under similar conditions [11,12]. This is also seen in the evolution of the surface areas compiled in Table 1. The values of surface area are quite low for the mixture allowed to react for 1-2 hours, but stabilize at around 450-500 m^2/g for longer periods; these are typical values reported in the literature for xerogels and aerogels [2-5, 11-14]. These observations indicate that most of the monomers have reacted at 4 and 12 hours, the latter being a timeframe similar to that reported for R-F aerogels with the same R/C molar ratio [26,27]. Hence we selected a timeframe of 4 hours for the gelation/aging step as the optimum value (in terms of texture development and time savings) for the synthesis of subsequent samples.

Fig. 4. Correlation between the gelation/aging time and temperature and the micro- mesopore volumes.

Fig. 2 shows the N_2 adsorption isotherms of the gels prepared by allowing the polycondensation reaction to proceed for 4 hours at different temperatures between 70 and 95ºC. As seen, all of the samples displayed prominent hysteresis loops (type H2) at relative pressures above 0.5, in agreement with the characteristics reported for colloidal gels prepared using high R/C ratio [2-5]. Again, the position of the hysteresis loop was about the same for all the samples, although it became wider and better-defined with rising the temperature. This indicates that the formation and growth of the clusters leading to the mesoporous void is controlled by the formulation of the xerogel (i.e., R/C, R/W, R/F molar ratios) rather than by the temperature of the gelation/aging step. Interestingly, the gels prepared at 85 and 90ºC displayed a wider hysteresis loop (expanded toward higher relative pressures) and a stepped desorption with an inflection point in the hysteresis loop at $p/p_o \sim 0.55$. Such two-step desorption pattern suggests that these materials have a heterogeneous pore network with cavities of different sizes [28,29]; hence the curvature in the desorption branch would correspond to either pore blocking or cavitation effects due to the consecutive emptying of the different pores of the system.

Differences concerning the total pore volumes and the micro to mesopore balance are also worth mentioning (Fig. 3, 4 and Table 1). Increasing the temperature of the gelation/aging step between 70-85ºC improved the textural features of the gels, particularly in the mesopore range, whereas the overall microporosity followed a more gradual trend. The CO_2 adsorption isotherms also corroborate that the effect of the gelation/aging temperature on the microporosity is almost negligible, since all the xerogels -with the exception of sample OG85- showed overlapping CO_2 adsorption isotherms (hence, similar characteristics).

Comparatively, the gel prepared at 70ºC displayed the lowest porosity of the series, indicating that this temperature is too low for the cross-linking of the monomers at a relatively fast rate to obtain a well connected porous structure in the timeframe used. In contrast, the pore volumes of the samples prepared at 85-90ºC were twice higher than those of OG70 (Table 1). The average mesopore width

also increased with temperature, reaching a maximum at 85 ºC as seen in Fig. 2C. Above this temperature, no further development of the porosity was obdserved, but rather a slight drop of the total pore volumes. The same tendency is observed for the ratio V_{meso}/V_{micro}, confirming the best development of the micro-mesoporous architecture at 85ºC.

As briefly described in the introduction, the sol-gel mechanism is initiated by the addition reaction of the R-F precursors and cluster growth [2]. Thus it seems that the addition reaction is controlled by the composition of the reaction mixture, whereas the rate of the clusters growth and cross-linking would depend on the temperature of the gelation/aging. This would explain why large differences are seen in the mesoporous structure, while the microporosity remains practically the same for the series prepared at different temperatures (Fig. 3). On the other hand, the slight deterioration of the porosity above 85ºC could be attributed to several factors such as the sudden heating of the solution (see experimental section), the fast evaporation rate of the aqueous medium at 90 and 95ºC, and the changes in the dissociation constants of water and resorcinol with temperature (hence modifying the pH). The latter facts could promote a phase demixing that would affect the development of porosity [30].

Further information on the textural features of the synthesized xerogels was obtained from the analysis of the PSDs using the 2D-NLDFT-HS model [22], applied to the desorption branch of the isotherm. The fitting of the model to experimental adsorption isotherms was very good for all the samples (Fig. S1 in the Supplementary File), confirming its validity for the characterization of these materials. Furthermore, BJH formulism (Fig. S2) yielded rather similar results in the mesopore range to those obtained by 2D-NLDFT-HS method, although the patterns in the former are shifted to higher values on the pore size scale due to the fact that BJH assumes cylindrical pore shape.

The cumulative and differential pore distribution curves confirmed the roles of the temperature and time during the gelation/aging step in the formation of the pore structure (Fig. 1B, 1C). For instance, the evolution of the microporosity and the enlargement of the mesopores are evident at long times (Fig. 1). On the other hand, the effect of the temperature in the PSD is less pronounced, with all the samples -with the exception of OG70- showing rather similar distribution of pore sizes (Fig. 2). Interestingly, the samples prepared at 85 and 90ºC showed a wider distribution in the mesopore range. This is more clearly seen in the hump appearing between 4-5 nm for OG85 in Fig. 1C, and is in agreement with the stepped pattern of the desorption branch of the isotherm due to a multimodal distribution of mesopores. As for microporosity, data obtained from 2D-NLDFT-HS was relatively close to the values obtained by the DR method (Table 1), corroborating again the validity of the method for the textural analysis of the organic xerogels.

The elemental analyses of the xerogels are shown in Table 2, along with the basic/acidic character evaluated by means of the pH_{PZC}. All the gels displayed oxygen contents above 30 wt.%; even though differences in composition are subtle, as a general rule the oxygen content of the gels decreased slightly with the gelation/aging time. Since the oxygen content depends on the cross-linking of the monomers [2, 30], this indicates that the cross-linking reaction is favored at long gelation/aging times.

A similar trend is observed for the temperature up to 85ºC. The samples prepared at 90 ºC and 95 ºC break this trend, likely due to the sudden heating of the aqueous solution at temperatures close to the boiling point of water, as mentioned above [30]. The organic gels presented a slightly acidic nature as seen in the trend of the values of the pH_{PZC} (Table 2).

Table 2. Elemental analysis and point of zero charge of the prepared materials.

3.2. Activation of the gels

According to literature, the gels prepared following a subcritical drying typically suffer from low mechanical resistance, particularly if the synthesis does not involve a solvent exchange process to eliminate the strong contractive forces that appear during evaporation of water from the pores, due to the high surface tension of water [2,26,27]. In agreement with those studies and since we have eliminated the solvent exchange step, the dried gels underwent a small shrinkage. These xerogels are expected to be structurally sensitive to further heat treatment at the high temperature, as opposed to mechanically stable aerogels [12]. To investigate the textural and structural stability of the materials synthesized by this accelerated route, one of the gels (sample OG80) was subjected to thermal treatment at high temperature and different atmospheres (ca. carbonization under inert atmosphere followed by activation in CO_2 and chemical activation in K_2CO_3) to obtain denser carbon gels. The corresponding N_2 and CO_2 adsorption isotherms are represented in Fig. 3 and 5, respectively, while the main textural parameters are collected in Table 1.

As seen, carbonization at 800ºC caused an important loss of the mesoporous structure accompanied by an increase in the micropore volume, also evidenced in the CO_2 adsorption isotherms. This is attributed to the strong interfacial tensions exerted on the R-F backbone during the evolution of volatiles (i.e., OH moieties, H_2O, CO_2, CO and other organic molecules) [4]. According to literature, this effect is generally more remarkable in gels prepared using low R/C ratio, but in our case (R/C of 200) we link it to the direct drying of the wet gels without a solvent exchange step. Further activation under CO_2 atmosphere of the carbonized gel resulted in the creation of and enlargement of the microporosity, in a similar pathway as that of any other carbon precursor [31]. However the mesopore structure lost during the carbonization is not recovered. The PSDs shown in Fig. 5 corroborated the large collapse of the mesoporous structure of the xerogels upon carbonization.

Fig. 5. (A) Nitrogen adsorption/desorption isotherms at -196 ºC for the series of carbonized and activated xerogels, and (B) cumulative and (C) derivative PSD curves calculated using 2D-NLDFT-HS method.

A different trend was obtained upon chemical activation; even though the treatment was also carried out at high temperature (i.e., 700ºC), the chemically activated gel displayed a type I/IV isotherm,

characteristic of a bimodal micro-mesopore system. Compared to the N_2 adsorptions isotherms of the carbonized and pristine samples, the hysteresis loop of CGCA is expanded to higher relative pressures (from 0.5 to 0.8), indicating the enlargement of the average mesopore size. The widening of the mesoporosity of CGCA is also shown in Fig. 5, as the pore size distribution expands from small to large mesopores. Thus, the structural collapse of the organic R-F gels prepared with low gelation/aging temperatures and time during thermal treatment can be counterbalanced by the chemical activation reaction, where the creation of new micropores is accompanied by the enlargement of the mesopore structure. The CO_2 adsorption isotherms of the chemically activated sample CGCA also corroborates the presence of a larger volume of micropores of smaller sizes compared to the sample prepared by physical activation (sample CGPA), despite the total pore volume and surface area are quite similar.

Elemental analysis confirmed the large loss of volatile matter (i.e., oxygen and hydrogen losses) during the thermal treatments at high temperature, with the oxygen contents decreasing from 30-35 wt.% down to and below 10 wt.% after pyrolysis or activation. The evolution of the volatiles caused the loss of the acidic character of the xerogels, with the carbonized and activated samples showing a marked hydrophobicity (being more evident in CG and CGPA). This contrasts with the slight acidic nature -evaluated by the values of the point of zero charge-, of the organic xerogels.

3.3. Energy cost assessment

Once evaluated the impact of the accelerated synthesis using mild polymerization conditions on the textural features of the xerogels, we have performed an energetic and cost assessment of our approach based on the energy consumption and the electric power needed in the overall process. For this purpose, we monitored the consumed energy by the conventional oven to reach and maintain the temperature during the gelation/aging and drying stages. Although the overall energy consumption will strongly depend on the specific set-up used (size and insulation of the oven, degree of filling) and has not been optimized for this study, we have maintained similar conditions (volume of sample treated) for all the tests, which allows direct comparison of the data and the assessment of the energy consumed during the gelation/aging process. The oven featured a linear correlation between the cumulated electric energy consumption and the adjusted set point temperature, which allowed to calculate the energy consumed according to this empirical equation:

$$Energy = \sum_i (1.688 \cdot T_i - 51) \cdot 10^{-3} \cdot t_i \quad i = \textit{gelation/aging step, drying step.} \qquad (1)$$

where E is the energy consumed in kilowatts per hour (kWh), T_i is the temperature (ºC) and t_i is the time (h) for each stage.

The calculated energy power consumed for each synthesis is compiled in Table 3; it is clear that the highest consumption is related to the final drying step as it is carried out at the highest temperature and

longer time. Increasing the gelation/aging temperature by 25ºC (from 70 to 95ºC) resulted in a two-fold increase in the energy consumed in this stage, whereas the improvement in the textural properties was not too high. Considering the energetic balance and the textural features of the xerogels, it is clear that the synthesis at 85ºC is the most advantageous one. Comparatively, the energy consumed for the conventional procedures at the same temperature but allowing the gelation/aging for 3-5 days would be 20 to 30 times higher that that reported in our approach.

To balance the textural properties of the xerogels with the energy power consumed, we have also calculated the production in terms of mass of xerogel per kilowatt hour considering an average yield of 17 grams of dried gel obtained for an initial volume of 50 mL. Then we have calculated the energetic cost for the development of the textural features in terms of surface area and mesopore volumes per kWh consumed. The calculated values are represented in Fig. 6.

Fig. 6. Correlation between the energy used for the synthesis of the xerogels and their surface area S_{BET} (left axis, stripped bars) and V_{meso} (right axis, solid blue bars).

Table 3. Energy consumed in kWh in the different steps of the synthesis in the conventional oven.

As seen, there is a different distribution of the energy consumed for the development of the textural features in the micro- and mesoporous range. For the lowest temperature the energy is mainly invested in increasing the surface area (i.e., microporosity). Above 85ºC, the energy is mainly used in the formation of mesoporosity, confirming that the kinetics of the addition and condensation reactions of is faster at this temperature, and thus the energy is mainly used for the aggregation of the clusters in large pores. Comparatively, Fig. 6 shows about 50% of energy savings if the gelation/aging stage is performed at 85 ºC compared to 70 or 95ºC, for a similar volume of mesopores

Finally, we have compared our results with those recently reported using microwave-assisted heating for the synthesis of organic gels [32,33]. The latter method has the advantage of a rapid heating of the precursor solution (a few seconds) to the desired temperature, compared to the time needed using convective heating in conventional ovens (in the order of minutes). Our data show that the accelerated syntheses using mild temperatures and short gelation/aging times are more favorable in terms of grams of xerogel per kWh of energy consumed for similar textural properties, at least at a laboratory scale. Additionally, conventional heating is easily scaled up for an increased production capacity.

Although the procedure is carried out at laboratory scale (only 10% of the capacity of the oven was used to produce 17 g of xerogels, and about 2 kg could have been produced with nearly the same energy consumption) and thus is yet far from been optimized from the viewpoint of obtaining the maximum amount of material with minimum energy consumption, the correlation between the energy consumed and the textural parameters can be a useful tool to optimize the synthesis of porous xerogels.

4. CONCLUSIONS

In this study, the conventional sol-gel polycondensation of R-F to obtain porous gels has been modified following an experimental approach based on mild conditions (low gelation/aging temperatures and times) to accelerate the synthesis and to reduce the energy costs. The results have shown that porous gels with well developed micro-mesoporous structures can be obtained within less than a day at moderate temperatures (85-90ºC), and omitting the solvent-exchange step before drying.

More importantly, the energy savings are similar to those obtained using microwave-heating in terms of grams of xerogel per kWh of energy consumed for similar textural properties. The correlation between the energy power consumed and the textural parameters is a useful tool to optimize the synthesis parameters balancing the energy costs with the micro-mesoporous architecture of the final materials.

Data have shown that the temperature of the gelation/aging step mainly affects the formation of the mesoporous structure, whereas the microporosity depends on the composition of the precursor's mixture. The omission of the solvent exchange stage yielded porous but fragile gels which mesoporous structure collapses upon carbonization at high temperature in inert atmosphere, due to the surface tensions applied to the backbone during drying and decomposition of volatiles. Further activation in CO_2 atmosphere did not allow the recovery of the mesoporous network. On the other hand, chemical activation in K_2CO_3 is a feasible alternative to counterbalance such structural deficiency of the organic xerogels, with the resulting activated materials displaying a bimodal micro-mesoporous distribution.

ACKNOWLEDGMENTS

The authors thank the financial support of the Spanish MINECO (grant CTM2011/023378) and Fondos Feder PCTI Asturias (grant PC10-002). EDIP and RJC are grateful to CONACyT and PCTI Asturias for the mobility grant (290674) and Severo Ochoa fellowship, respectively. COA acknowledges Dr. Jacek Jagiello for the fruitful discussion on 2D-NLDFT-HS model.

REFERENCES

[1] F. Schüth, K.S.W. Sing, J. Weitkamp, Handbook of porous solids, first ed., Wiley-VCH, New York, 2002.

[2] S.A. Al-Muhtaseb, J.A. Ritter, Adv. Mater. 15 (2003) 101-114.

[3] A.M. ElKhatat, S.A. Al-Muhtaseb, Adv. Mater. 23 (2011) 2887-2903.

[4] N. Job, R. Pirard, J. Marien, J.-P. Pirard, Carbon 42 (2004) 619-628.

[5] N. Job, A. Thery, R. Pirard, J. Marien, L. Kocon, J.N. Rouzaud, F. Beguin, J.-P. Pirard, Carbon 43 (2005) 2481-2494.

[6] T. Yamamoto, A. Endo, T. Ohmori, M. Nakaiwa, Carbon 42 (2004) 1671-1676.

[7] C. Moreno-Castilla, F. Maldonado-Hódar, Carbon 43 (2005) 455-465.

[8] G. Pajonk, Appl. Catal. 72 (1991) 217-266.

[9] R. Pekala, J. Farmer, C. Alviso, T. Tran, S. Mayer, J. Miller, B. Dunn, J. Non-Cryst. Solids 225 (1998) 225, 74-80.

[10] L.L. Zhang, X. Zhao, Chem. Soc. Rev. 38 (2009) 2520-2531.

[11] E. Calvo, C.O. Ania, L. Zubizarreta, J. Menéndez, A. Arenillas, Energy Fuels 24 (2010) 24 3334-3339.

[12] M. Haro, G. Rasines, C. Macias, C.O. Ania, Carbon 49 (2011) 3723-3730.

[13] J. Farmer, D. Fix, G. Mack, R. Pekala, J.Poco, J. Appl. Electrochem. 26 (1996) 1007-1018.

[14] R.W. Pekala, J. Mater. Sci. 24 (1989) 3221–3227.

[15] H. Tamon, H. Ishizaka, T. Araki, M. Okazaki, Carbon 36 (1998) 1257-1262.

[16] K. Kraiwattanawong, S.R. Mukai, H. Tamon, A.W. Lothongkum, Microporous Mesoporous Mater. 98 (2007) 258-266.

[17] T.P. Fellinger, R.J. White, M.M. Titirici, M. Antonietti, Adv. Funct. Mater. 22 (2012) 3254-3260.

[18] H. Pröbstle, C. Schmitt, J. Fricke, J. Power Sources 105 (2002) 189-194.

[19] S. Berthon, O. Barbieri, F. Ehrburger-Dolle, E. Geissler, P. Achard, F. Bley, A.-M. Hecht, F. Livet, G.M. Pajonk, N. Pinto, J. Non-Cryst. Solids 285 (2001) 154-161.

[20] N. Job, F. Panariello, M. Crine, J.-P. Pirard, A. Leonard, Colloids Surf., A: Physicochem. Eng. Aspects 293 (2007) 224-228.

[21] C. Lin, J. Ritter, Carbon 35 (1997) 1271-1278.

[22] J. Jagiello, J.P. Olivier, Adsorpt. 19 (2013) 777–783.

[23] M.S. Contreras, C.A Paez, L. Zubizarreta, A. Leonard, S. Blacher, C.G. Olivera-Fuentes, A. Arenillas, J.-P. Pirard, N. Job, Carbon 48 (2010) 3157-3168.

[24] J. Noh, J.A. Schwarz, J. Colloid Interf. Sci. 130 (1989) 157-164.

[25] U. Fischer, R. Saliger, V. Bock, R. Petricevic, J. Fricke, J. Porous Mater. 4 (1997) 281-285.

[26] R.W. Pekala, F.M. Kong, Proc. 2nd Int. Symposium on Aerogels, Montpellier, France,1989, p. C4.5

[27] M. Wiener, G. Reichenauer, T. Scherb, J. Fricke, J. Non-Cryst. Solids 350 (2004) 126-130.

[28] D.H. Everett, F.S. Stone (Eds.), The Structure and Properties of Porous Materials, Butterworths, 1958, pp. 84-145.

[29] A. Vishnyakov, A.V. Neimark, Langmuir 19 (2003) 3240-3247.

[30] N. Job, F. Panariello, J. Marien, M. Crine, J.-P. Pirard, A. Léonard, J. Non-Cryst. Solids 352 (2006) 24-34.

[31] F. Rodriguez-Reinoso, H. Marsh, Activated Carbon, first ed., Elsevier, Oxford, 2006.

[32] E. Calvo, E. Juárez-Pérez, J. Menéndez, A. Arenillas, J. Colloid Interf. Sci. 357 (2011) 541-547.

[33] E. Juárez-Pérez, E. Calvo, A. Arenillas, J. Menéndez, Carbon 48 (2010) 3305-3308.

Figures Captions

Fig. 1. (A) Nitrogen adsorption/desorption isotherms at -196 ºC for the series of xerogels prepared by gelation/aging at 70 ºC during different times; (B) cumulative and (C) derivative PSD curves calculated using 2D-NLDFT-HS method.

Fig. 2. (A) Nitrogen adsorption/desorption isotherms at -196 ºC for the series of xerogels prepared by gelation/aging at different temperatures for 4 hours; (B) cumulative and (C) derivative PSD curves calculated using 2D-NLDFT-HS method.

Fig. 3. CO_2 adsorption isotherms at 0 ºC for the series of synthesized xerogels.

Fig. 4. Correlation between the gelation/aging time and temperature and the micro- mesopore volumes.

Fig. 5. (A) Nitrogen adsorption/desorption isotherms at -196 ºC for the series of carbonized and activated xerogels, and (B) cumulative and (C) derivative PSD curves calculated using 2D-NLDFT-HS method.

Fig. 6. Correlation between the energy used for the synthesis of the xerogels and their surface area S_{BET} (left axis, stripped bars) and V_{meso} (right axis, solid blue bars).

Tables Captions

Table 1. Porosity parameters obtained from the N_2 adsorption isotherms at -196 ºC for the xerogels.

Table 2. Elemental analysis and point of zero charge of the prepared materials.

Table 3. Energy consumed in kWh in the different steps of the synthesis in the conventional oven.

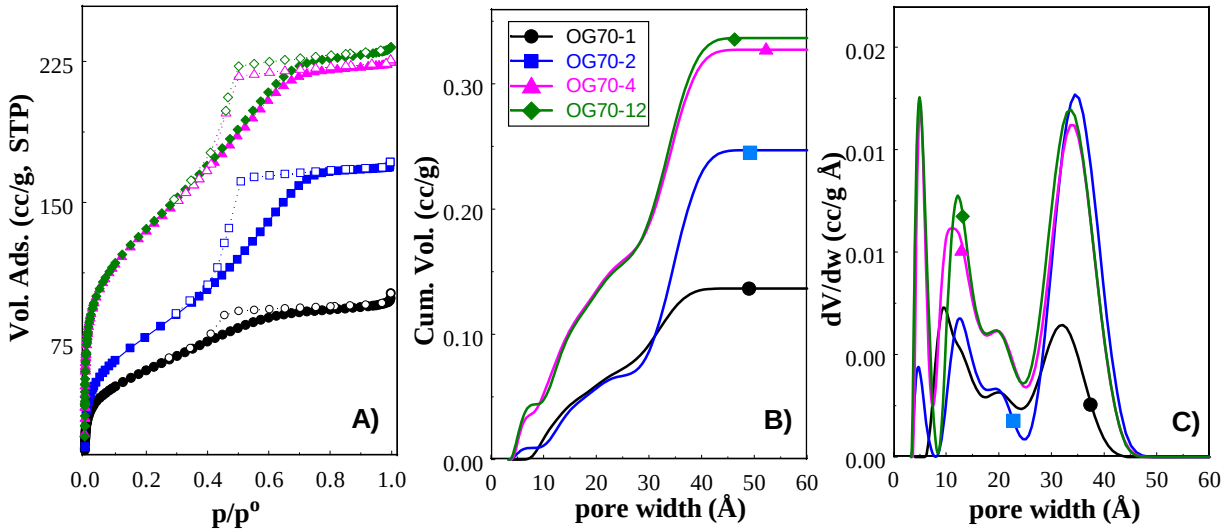

Fig. 1. (A) Nitrogen adsorption/desorption isotherms at -196 ºC for the series of xerogels prepared by gelation/aging at 70 ºC during different times; (B) cumulative and (C) derivative PSD curves calculated using 2D-NLDFT-HS method.

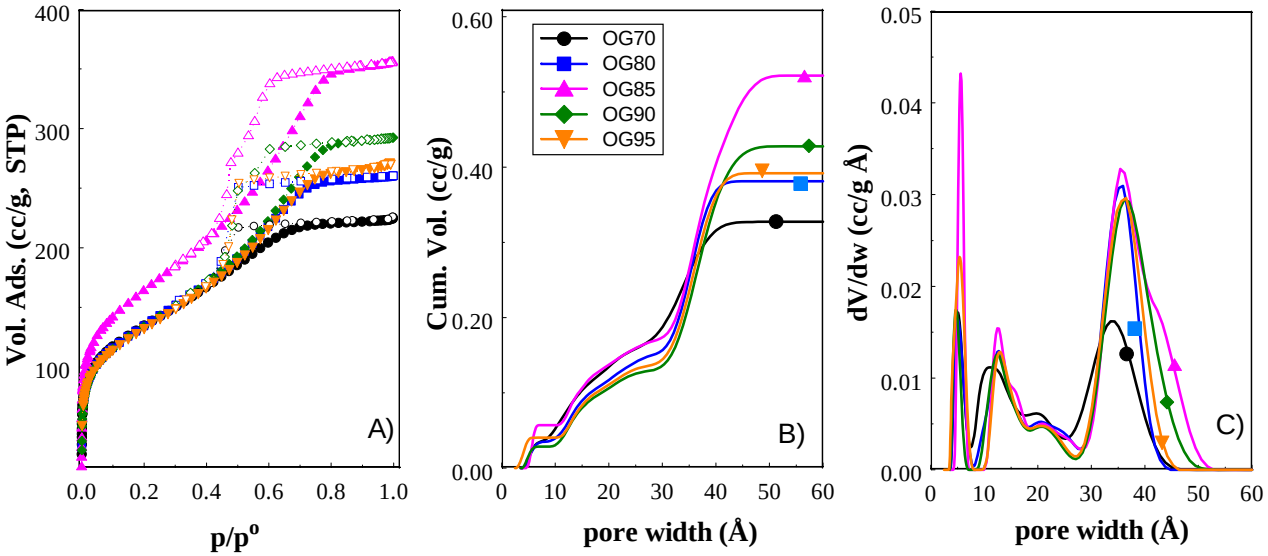

Fig. 2. (A) Nitrogen adsorption/desorption isotherms at -196 ºC for the series of xerogels prepared by gelation/aging at different temperatures for 4 hours; (B) cumulative and (C) derivative PSD curves calculated using 2D-NLDFT-HS method.

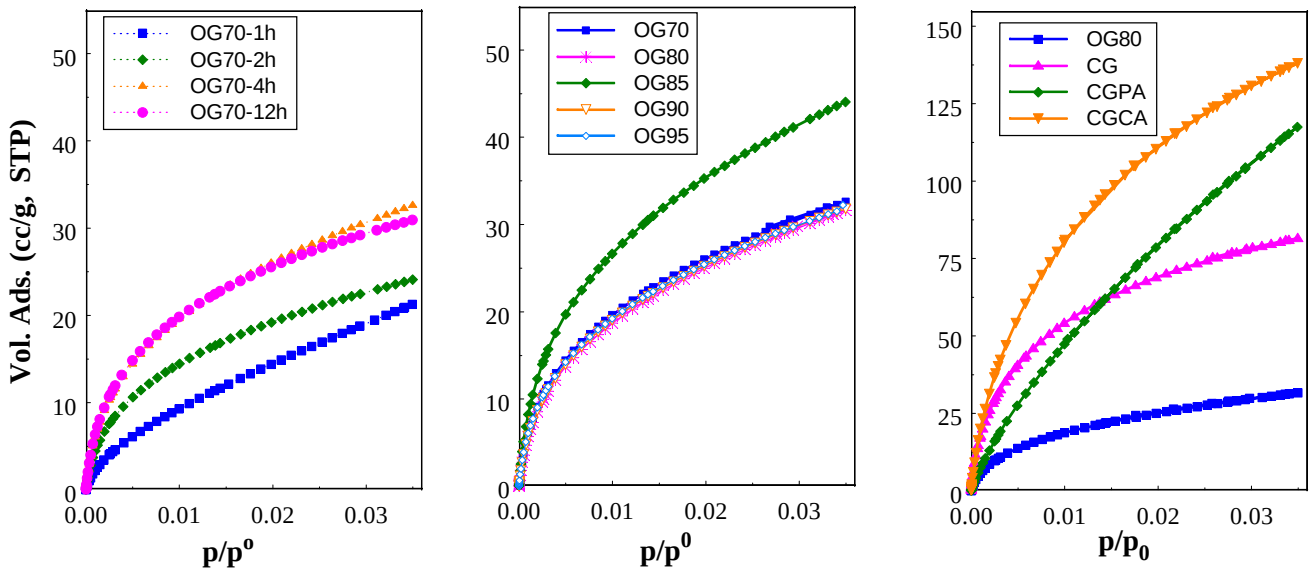

Fig. 3. CO_2 adsorption isotherms at 0 ºC for the series of synthesized xerogels.

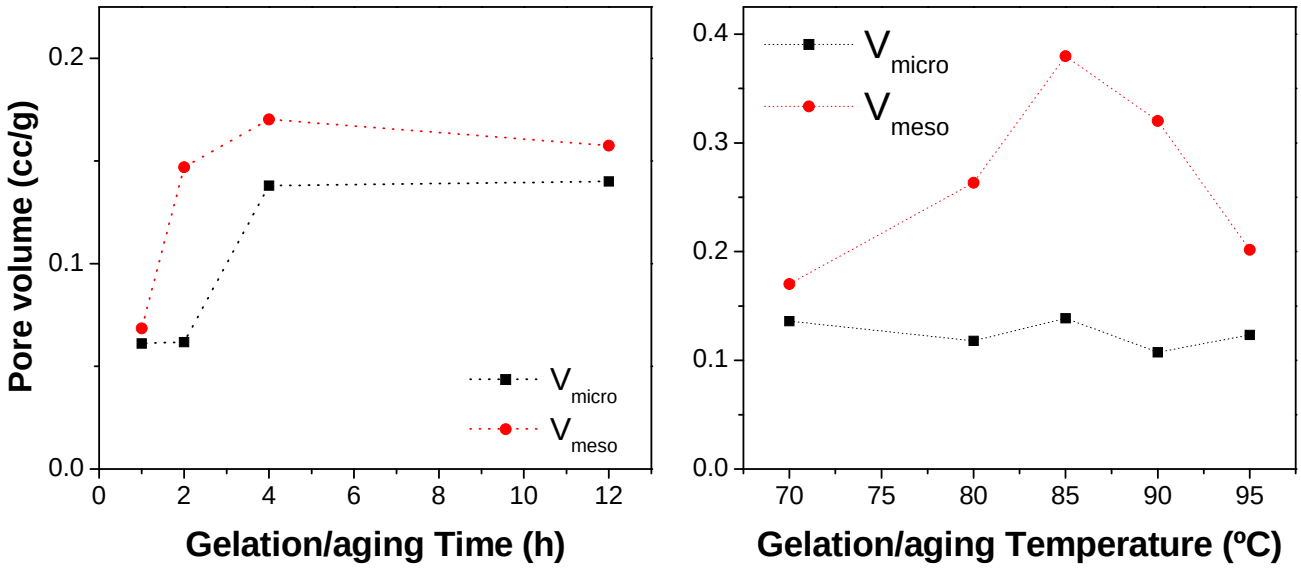

Fig. 4. Correlation between the gelation/aging time and temperature and the micro- mesopore volumes.

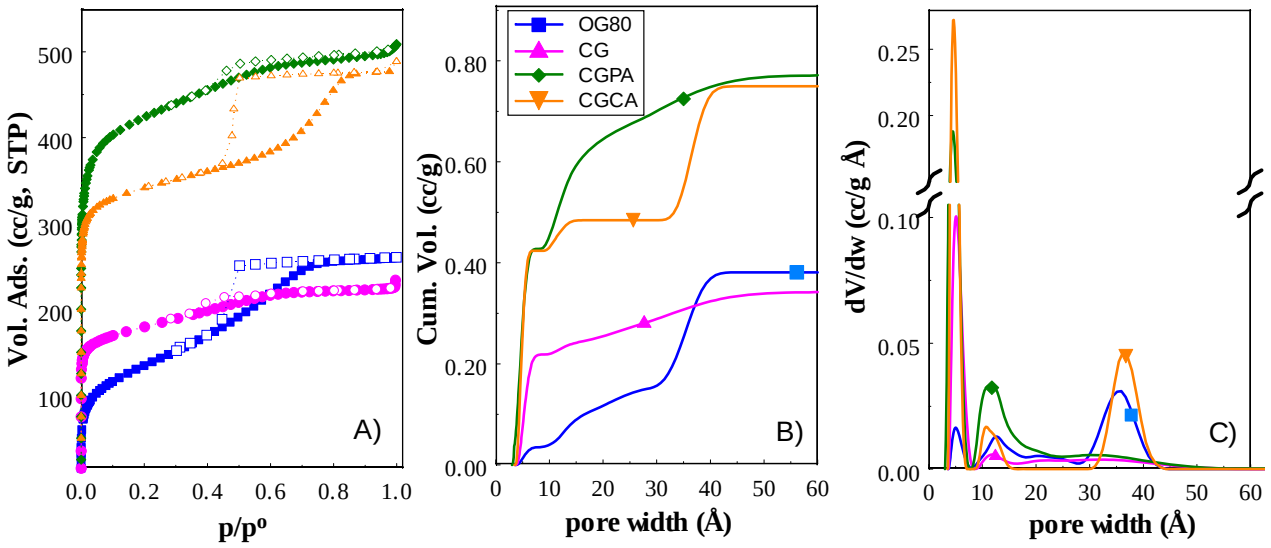

Fig. 5. (A) Nitrogen adsorption/desorption isotherms at -196 ºC for the series of carbonized and activated xerogels, and (B) cumulative and (C) derivative PSD curves calculated using 2D-NLDFT-HS method.

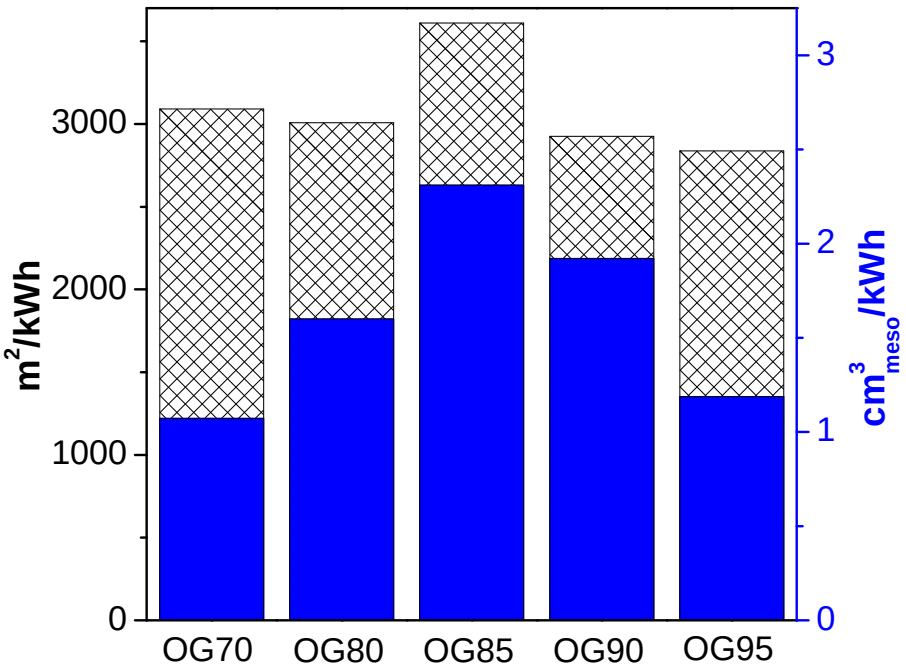

Fig. 6. Correlation between the energy used for the synthesis of the xerogels and their surface area S_{BET} (left axis, stripped bars) and V_{meso} (right axis, solid blue bars).

Table 1. Porosity parameters obtained from the N_2 adsorption isotherms at -196 ºC for the xerogels.

	ρHe (g/cc)	ρ_{Bulk} (g/cc)	S_{BET} (m^2/g)	V_{TOTAL} (cc/g) [A]	Wo, MICRO (cc/g) [B]	V_{MICRO} (cc/g) [C]	V_{MESO} (cc/g) [C]	Ratio V_{micro}/V_{meso} [C]
OG70-1	1.42	1.17	220	0.15	0.08	0.06	0.07	0.89
OG70-2	1.43	1.01	287	0.29	0.09	0.06	0.15	0.42
OG70-4	1.42	0.95	490	0.35	0.15	0.14	0.17	0.81
OG70-12	1.43	0.97	445	0.33	0.12	0.13	0.16	0.81
OG80	1.49	0.92	489	0.41	0.16	0.12	0.26	0.45
OG85	1.41	0.79	594	0.55	0.17	0.14	0.38	0.37
OG90	1.42	0.87	487	0.45	0.15	0.11	0.32	0.34
OG95	1.44	0.90	478	0.42	0.16	0.12	0.20	0.61
CG	1.51	0.96	682	0.38	0.24	0.26	0.08	3.10
CGPA	2.19	0.81	1640	0.78	0.57	0.62	0.12	5.10
CGCA	2.09	0.81	1332	0.75	0.50	0.49	0.26	1.70

[A] total pore volume evaluated at p/p_0 ~0.99

[B] evaluated from DR method

[C] evaluated from 2D-NLDFT-HS

Table 2. Elemental analysis and point of zero charge of the prepared materials

	C (wt.%)	H (wt.%)	O (wt.%)	pH_{PZC}
OG70-1	60.8	5.6	33.6	3.5
OG70-2	61.8	4.9	33.3	3.6
OG70-4 (OG70)	63.8	4.3	31.8	3.8
OG70-12	64.0	4.7	31.2	3.8
OG80	64.5	4.5	30.9	3.7
OG85	65.5	4.5	30.0	4.4
OG90	64.0	4.3	31.6	3.6
OG95	62.5	4.3	33.1	4.0
CG	96.4	0.6	3.1	9.9
CGPA	89.9	0.6	9.5	7.8
CGCA	98.0	0.4	1.7	11.6

Table 3. Energy consumed in kWh in the different steps of the synthesis in the conventional oven.

	Gelation/aging step	Drying step (150ºC, 12h)	Total consumption
OG70-1	0.07	2.43	2.49
OG70-2	0.13	2.43	2.56
OG70-4 (OG70)	0.27	2.43	2.70
OG70-12	0.81	2.43	3.23
OG80	0.34	2.43	2.76
OG85	0.37	2.43	2.80
OG90	0.40	2.43	2.83
OG95	0.44	2.43	2.86

Supporting Information

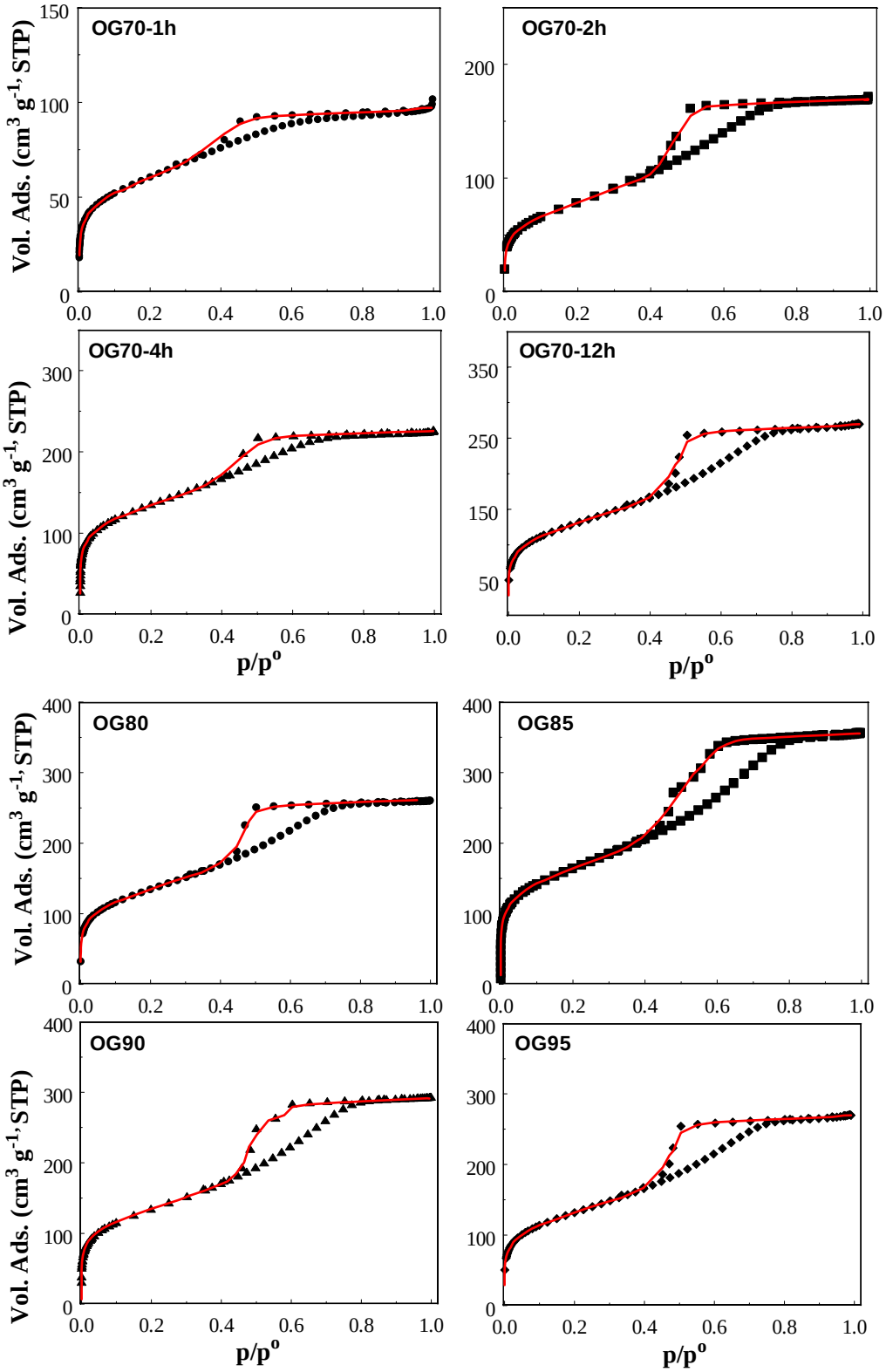

Fig. S1 Fitting (lines) of experimental isotherms (symbols) by the 2D-NLDFT-HS model on the studied xerogels.

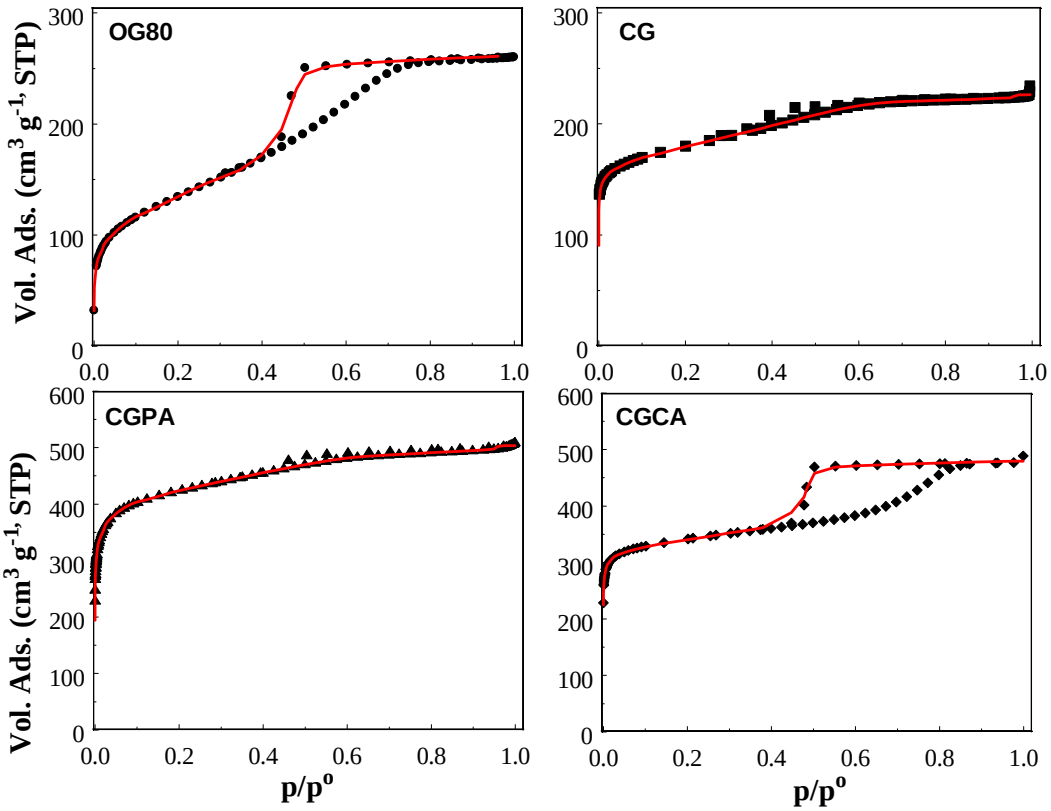

Fig. S1 (cont) Fitting (lines) of experimental isotherms (symbols) by the 2D-NLDFT-HS model on the studied xerogels.

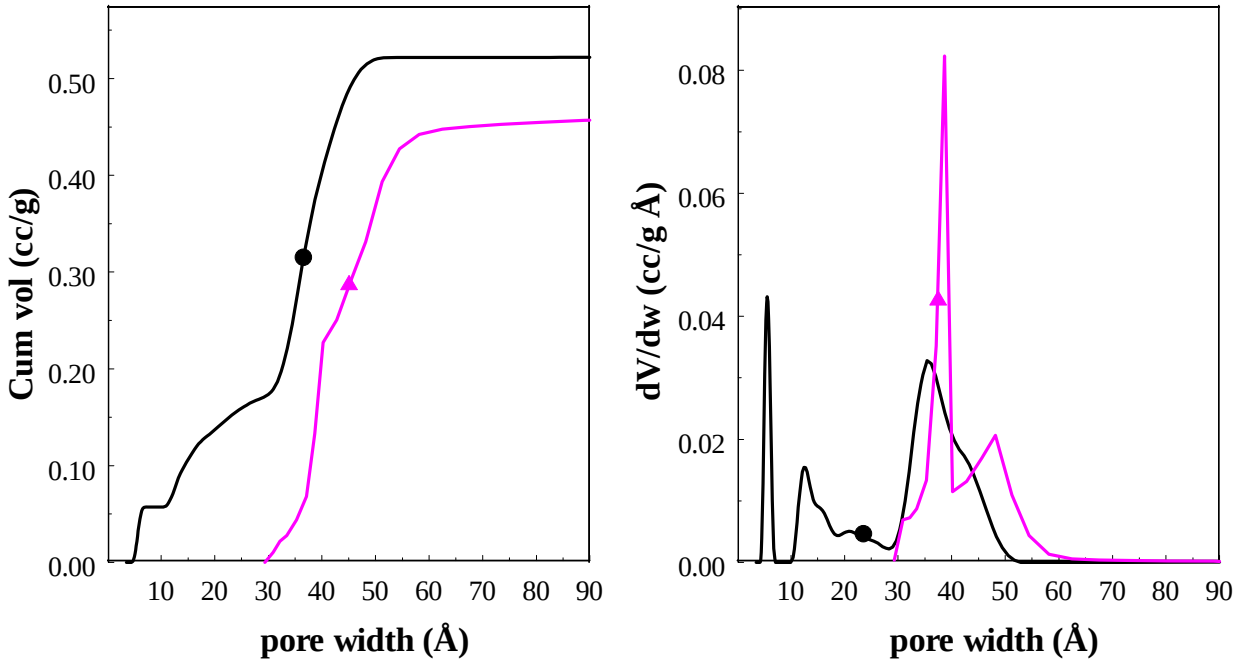

Fig. S2 Comparison of the PSD curves obtained using the 2D-NLDFT-HS model (circle) and BJH formulism (triangle) applied to sample OG85.